Research Article | Vol. 26, No. 17 | 20 Aug 2018 | OPTICS EXPRESS 22307

Optics EXPRESS

Humidity-induced Brillouin frequency shift in perfluorinated polymer optical fibers

ANDY SCHREIER,* ALEKSANDER WOSNIOK, SASCHA LIEHR, AND KATERINA KREBBER

Bundesanstalt für Materialforschung und -prüfung (BAM), Unter den Eichen 87, 12205 Berlin, Germany
**andy.schreier@bam.de*

Abstract: We report, to our knowledge, for the first time on humidity-induced Brillouin frequency shifts in perfluorinated graded index polymer optical fibers. A linear relation between Brillouin frequency shift and humidity was observed. Furthermore, the humidity coefficient of the Brillouin frequency shift is demonstrated to be a function of temperature (-107 to -64 kHz/%r.h. or -426 to -49 kHz m^3/g in the range of 20 to 60 °C). An analytical description proves temperature and humidity as two mutually independent effects on the Brillouin frequency shift.

1. Introduction

Stimulated Brillouin scattering (SBS) in silica optical fibers has been intensively studied for several decades [1, 2]. The acquired knowledge has been successfully applied in fields of signal processing [3], THz signal generation [4], phase conjugation [5], lasing [6] and optical storage [7]. Applications for distributed strain and temperature sensing based on SBS in silica optical fibers were investigated intensively [8, 9]. The approach of SBS measurements in polymer optical fibers (POFs) as sensors is rather new [10]. In contrast to silica optical fibers, POFs offer higher break down strain [11], higher sensitivity to temperature and lower sensitivity to strain [12]. Hence, distributed temperature and strain fiber sensors based on SBS have been demonstrated in commercially available perfluorinated graded index POF (PFGI-POF), based on the frequency domain [13] or correlation domain approach [14, 15].

In all SBS sensors the Brillouin frequency shift (BFS) depends on temperature and strain. The sensitivity of PFGI-POF to humidity has been demonstrated [16]. However, the influence of humidity on the BFS needs to be investigated. Usually, state of the art humidity sensors are based on absorption loss measurements [17] or fiber Bragg grating wavelength shifts in silica optical fibers [18, 19] and in POFs [20, 21]). Additionally, humidity sensitive polymers were suggested as coatings for silica optical fibers, causing humidity-induced losses [17, 22]. However, apart of polyimide coated silica optical fibers [18, 23], commercially available silica optical fibers are less sensitive to humidity [24, 25]. In terms of POF, polymethylmethacrylate (PMMA) based fibers were proposed for humidity sensing [26]. Recently, a PMMA-POF sensor for distributed humidity sensing was demonstrated, based on Rayleigh scattering and absorption measurement at two wavelengths [27].

This paper presents the first results of the BFS sensitivity to humidity in commercially available PFGI-POFs. It is well known that most of common polymers exhibit affinity for water [28–30]. Thus, a water-induced swelling of the materials causes a change in their optical and mechanical properties [16, 31]. The used PFGI-POF consists of cyclic transparent optical polymer (CYTOP) as core material and polycarbonate as coating material. CYTOP is known for its low water absorption in contrast to polycarbonate [28, 32, 33]. Nevertheless, considerable attenuation changes caused by water absorption in the core material of the PFGI-POF have been demonstrated [16]. Additionally, it was shown that humidity has a profound effect during the annealing process in PMMA-POFs [30]. In this paper we show that PFGI-POF is less sensitive to humidity compared to PMMA-POF and the BFS to be a function of humidity.

#331960 https://doi.org/10.1364/OE.26.022307
Journal © 2018 Received 17 May 2018; revised 13 Jul 2018; accepted 18 Jul 2018; published 14 Aug 2018

Optics EXPRESS

2. Experimental

Humidity is the amount of water vapor in the air and is measured as absolute or relative humidity. Absolute humidity gives the water content of air expressed in g/m^3. In contrast, relative humidity represents the absolute humidity relative to the saturation vapor pressure for a specific temperature in %r.h.. The saturation vapor pressure e_w is a function of temperature T and is approximately given by the improved Magnus form in Eq. (1) [34].

$$e_w(T) = 6.1094 \cdot exp\left\{\frac{17.625 \cdot T}{243.04 + T}\right\} \tag{1}$$

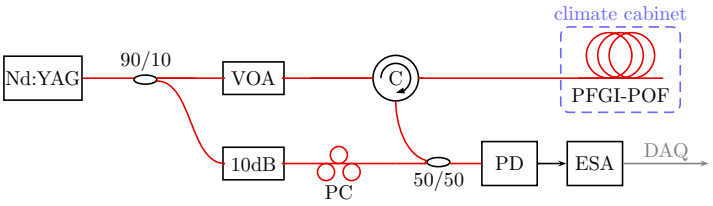

Fig. 1. Experimental setup for investigating the influence of humidity on BFS. Nd:YAG: solid state laser at 1319 nm, VOA: variable optical attenuator, C: circulator, PFGI-POF: 200 m fiber under test, 10dB: 10 dB fixed attenuator, PC: polarization controller, PD: photo diode, ESA: electrical spectrum analyser, DAQ: data acquisition.

Figure 1 displays the experimental setup. The used neodymium-doped yttrium aluminium garnet (Nd:YAG) laser has a linewidth of 5 kHz at a wavelength of 1319 nm. As described in [35], this laser is well suited to generate SBS in PFGI-POF. The laser output power of 22 dBm was split into two paths with a ratio of 90/10 (pump path / local oscillator path). The less powerful path was used as a local oscillator for the heterodyne detection. For this reason, the power in the local oscillator path was additionally attenuated by 10 dB and polarization controlled to maximize the SBS power level in each measurement. The input power at the 50/50 coupler was 2.6 dBm.

The pump path power was adjusted by a variable optical attenuator (VOA) and injected into a 200 m PFGI-POF (GigaPOF-50SR by Chromis Fiberoptics) after passing the circulator. The optical beat signal of backscattered Stokes light from the PFGI-POF and local oscillator path was detected by a photo diode (PD). The beat spectrum was measured by an electrical spectrum analyzer (ESA). All ESA measurements were performed at a resolution bandwidth of 300 kHz, a spectral resolution of 1.6 MHz and an averaging of 1000 samples.

All optical paths are standard single mode silica fibers with a core diameter of 8.2 μm, excepting the fiber under test (PFGI-POF). As described in [36, 37], the maximum SBS power level is generated by injecting the laser light into the fundamental mode of the PFGI-POF. In order to realize the required accurate coupling, APC connectors were used in our setup. Consequently, the presented Brillouin gain spectra are dominated by fundamental mode scattering, due to mode selective coupling. Though, the influence of higher optical modes on the measurement signal can not be excluded due to the strong mode coupling of the PFGI-POF [38]. In contrast to reported results [39], our fiber under test was longer (200 m). Detecting longer PFGI-POF is possible by operating at shorter wavelength (1319 nm), which offers the advantage of lower attenuation (30-35 dB/km [33]). The total loss along the PFGI-POF at 1310 nm was measured to be 6.5 dB, which is consistent with reported propagation loss for this wavelength. The insertion losses measured at the SMF-POF and POF-SMF interfaces are 0.14 dB and 7.67 dB, respectively. The measured losses are comparable to the reported values in [13] and the analytical model presented in [40].

Optics EXPRESS

To prevent a strain-induced BFS (-121.8 MHz/% for 1550 nm [12]), the PFGI-POF was placed on a 1 cm thick polyvinylchlorid plate. In order to remove any residual stress generated during the fiber manufacturing and to avoid fiber shrinkage, a long-term fiber annealing was performed for 72 hours at 70 °C and 95 % relative humidity (r.h.) [30, 41].

After annealing, all Brillouin gain spectra (BGSs) were measured at constant temperatures under variation of the relative humidity. Within each cycle the relative humidity was increased from 20 %r.h. to 95 %r.h. and subsequently decreased using the same steps. The diffusion of water into polymers is a relatively slow entropy-driven process [30, 31] This process depends on the relative humidity and temperature of the environment [31]. In order to achieve a homogeneous water distribution within the fiber, all BGS measurements were performed after 12 hours of exposure time in between each step.

The investigations were carried out by using a Vötsch VCL4006 climate cabinet. The measurement uncertainty of temperature and relative humidity within a two-minute time window are determined to be $\Delta T = \pm 0.05$ K and $\Delta h = \pm 0.1$ %, respectively.

3. Results and discussion

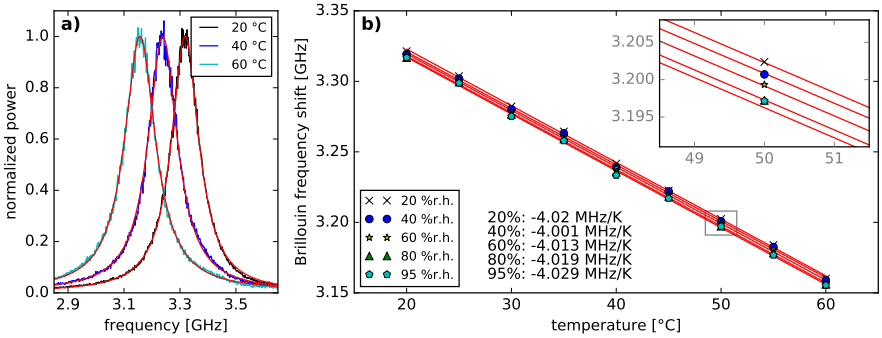

Fig. 2. a) BGS at 60 %r.h. for selected temperatures. b) Brillouin frequency shift as a function of temperature at specified relative humidity values. The corresponding linear regression functions are shown as well as an inset providing a closer view of the data set around 50 °C.

The BGS at each humidity step was averaged from 10 single measurements, in order to minimize the influence of the climate cabinet's temperature uncertainty on the extracted BFS. From each mean BGS point its corresponding noise level was subtracted. The noise was dominated by relative intensity noise, due to the high power of the local oscillator path. Subsequently, a Lorentzian regression function was computed to determine the BFS. Figure 2(a) shows normalized measurement data and their corresponding Lorentzian regression function at different temperatures.

Figure 2(b) displays the BFS as a function of temperature and the calculated temperature BFS coefficient C_T for all measured relative humidity steps. A linear relation between BFS and temperature for fixed relative humidities was observed. The temperature coefficient of BFS at 1319 nm pump wavelength is determined to be C_T = (-4.016 ±0.015) MHz/K, which is close to C_T = -3.2 MHz/K at 1550 nm [42]. Additionally, this coefficient exhibits no significant changes for variation of relative humidities. Hence, the temperature coefficient of BFS C_T can be considered to be independent of humidity influences.

Even though the humidity does not influence the temperature coefficient of BFS C_T, a BFS offset between each linear regression function was observed. This humidity dependent behavior

Optics EXPRESS

of BFS in polymer optical fibers has not been reported yet. However, the humidity-induced changes of the polymers in the PFGI-POF should be further investigated.

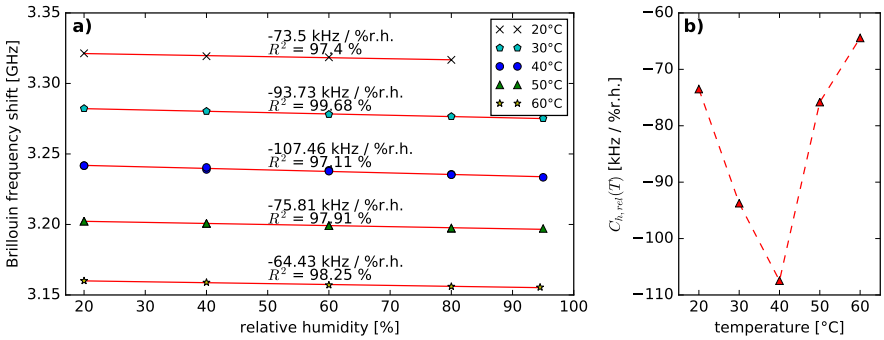

Fig. 3. a) Brillouin frequency shift as a function of relative humidity at selected temperatures and their corresponding linear regression function. The maximum observed uncertainty of the calculated slope values was ± 2.91 kHz/%r.h. b) Computed relative humidity coefficient of BFS $C_{h,rel}(T)$ as a function of temperature.

The BFS data sets of Fig. 2(b) are plotted as a function of relative humidity in Fig. 3(a) as well as the corresponding relative humidity coefficients of BFS $C_{h,rel}$. Within each isothermal step, a linear relation between BFS and relative humidity was observed. The computed $C_{h,rel}$ values as a function of temperature are plotted in Fig. 3(b). This figure shows, that $C_{h,rel}$ has different behavior in different temperature ranges (below 40 °C the coefficient decreases and above 40 °C it increases).

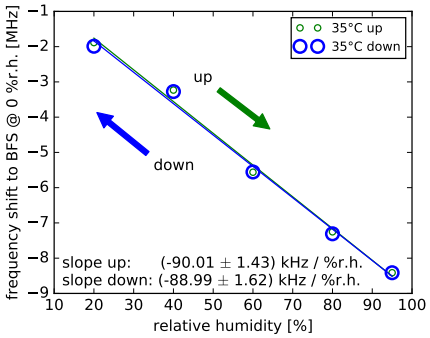

Fig. 4. Brillouin frequency shift plotted against relative humidity at 35 °C. The humidity was increased and decreased in order to observe a BFS hysteresis. Note that the frequency shift is given as a difference to the theoretical BFS at T = 35°C and h = 0 %r.h..

Furthermore, the BFS hysteresis behavior under variation of humidity was studied more closely. Fig. 4 displays the measured BFSs within the humidity cycle for 35 °C, separately. The observed small BFS fluctuations are within our measurement uncertainty of ΔBFS = ± 201 kHz ($\Delta BFS = \Delta T \cdot C_T$). Additionally, irrespective of the direction of the humidty change, the BFS exhibited a comparable slope of 89.5 kHz/%r.h.. Thus, no BFS hysteresis caused by humidity changes was observed.

As described earlier, C_T can be assumed to be independent of humidity influences, although the humidity evidently adds a separate BFS. Consequently, the BFS can be analytically described

Optics EXPRESS

as follows:

$$BFS(T,h) = C_h(T) \cdot h + C_T \cdot T + BFS_0 \tag{2}$$

BFS is the Brillouin frequency shift, h represents the humidity in % or g/m^3 and T the temperature in °C. BFS_0 is the theoretical BFS at $T = 0°C$ and $h = 0$ %r.h. in Hz. However, the dependence of $C_{h,rel}$ on temperature is a non-monotone function (see Fig. 3(b)). We converted the BFS as a function of relative humidity from Fig. 3(a) into BFS against absolute humidities by using the improved Magnus form [34], the molecular weight of water vapor (18.016 kg kmol^{-1} [43]) and the universal gas constant (8314.4 J kmol^{-1} K^{-1} [44]). The BFS is plotted against absolute humidity in Fig. 5(a). In contrast to the relative humidity, the BFS coefficients over absolute humidity $C_{h,abs}$ can be described by a monotonous function in the whole measured temperature range. Furthermore, the applied linear regression functions also indicate a linear relation between BFS and humidity in each isothermal step.

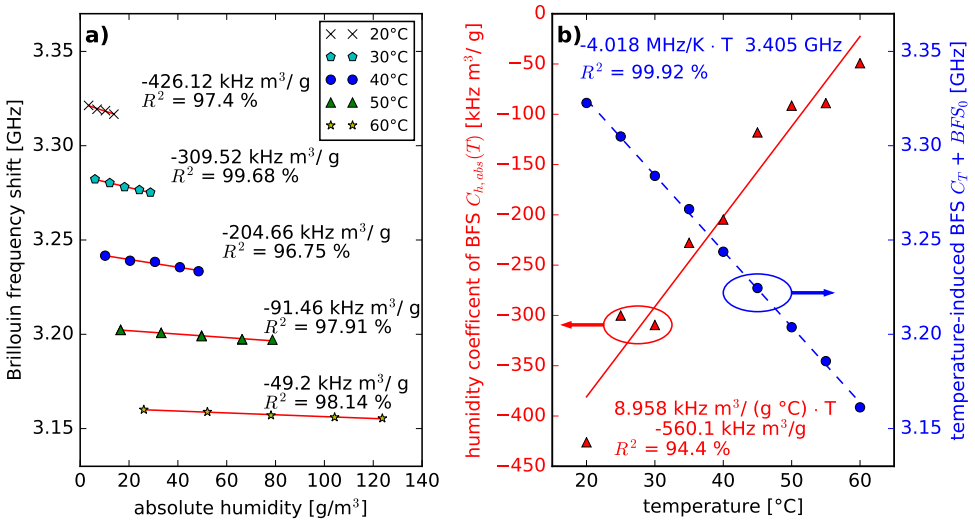

Fig. 5. a) Brillouin frequency shift as a function of absolute humidity at selected temperatures. b) Absolute humidity and temperature-induced Brillouin frequency shifts at all measured temperatures.

Taking into account the measurement data of Fig. 5(a), the parameters C_T, $C_h(T)$ and BFS_0 can be calculated. A linear regression function was computed for each isothermal measurement step. The intercepts of those linear functions refer to a humidity value of $h = 0$ g/m^3. Therefore, the intercepts describe the temperature-induced BFS only, which are plotted in Fig. 5(b) (see blue circles). C_T and BFS_0 refer to the parameters of a linear regression function of the intercept points (see blue dashed line as well as Eq. (3) and Eq. (4)). In contrast, the slopes of the linear regression functions in Fig. 5(a) describe the humidity coefficient of the BFS $C_h(T)$ (see red triangles in Fig. 5(b)). The linear regression function of the slopes is given in Eq. (5).

$$C_T = (-4.02 \pm 0.01)\ \text{MHz/K} \tag{3}$$

$$BFS_0 = (3404.8 \pm 0.5)\ \text{MHz} \tag{4}$$

$$C_h(T) = C_{h,abs}(T) = 8.96\ \text{kHz m}^3\ /\ (\text{g °C}) \cdot T\ - 560.1\ \text{kHz m}^3/\text{g} \tag{5}$$

Thus, by using Eq. (2) and the empirically determined values of $C_h(T)$, C_T and BFS_0, a BFS can be estimated for a given temperature and absolute humidity value. Furthermore, the

Optics EXPRESS

analytical description proves that temperature and humidity influence the BFS independently. Hence, a clear distinction between temperature and humidity is not possible by only measuring the BFS. In general, the BFS in PFGI-POF demonstrates a higher humidity sensitivity compared to reported humidity-induced BFSs in silica fibers at the same temperatures of 25 °C, 30 °C and 50 °C [24, 25].

4. Conclusion

This paper presents the first results of the humidity-induced BFS in PFGI-POF. The BFS was measured under variation of humidity and temperature. The effect of humidity on the BFS is clearly demonstrated, since a linear relation between Brillouin frequency shift and humidity was observed. The humidity coefficient of the BFS is demonstrated to be a function of temperature (-107...-64 kHz/%r.h. or -426...-49 kHz m^3/g in the range of 20...60 °C). Furthermore, an analytical description enables an estimation of BFS for specified temperature and humidity and proves temperature and humidity as two mutually independent effects on the BFS. A humidity-induced BFS hysteresis in PFGI-POF was not found. In addition the temperature coefficient of BFS at 1319 nm is determined to be $C_T = -4.02$ MHz/K and can be considered to be independent of humidity influences. The BFS is a function of both, temperature and humidity. This has to be considered in all POF-based SBS sensors.

Funding

PhD-program of Bundesanstalt für Materialforschung und -prüfung (BAM).

Acknowledgments

A special thanks to our colleagues from BAM Pavol Stajanca and Marcus Schukar for fruitful discussion and help.

Disclosures

The authors declare that there are no conflicts of interest related to this article.

References

1. G. P. Agarwal, *Nonlinear Fiber Optics* (Academic Press San Diego, CA, 2007).
2. T. Schneider, *Nonlinear Optics in Telecommunications* (Springer Science & Business Media, 2013).
3. S. Chin, L. Thévenaz, J. Sancho, S. Sales, J. Capmany, P. Berger, J. Bourderionnet, and D. Dolfi, "Broadband true time delay for microwave signal processing, using slow light based on stimulated Brillouin scattering in optical fibers," Opt. Express **18**, 22599–22613 (2010).
4. S. Preußler, N. Wenzel, R.-P. Braun, N. Owschimikow, C. Vogel, A. Deninger, A. Zadok, U. Woggon, and T. Schneider, "Generation of ultra-narrow, stable and tunable millimeter-and terahertz-waves with very low phase noise," Opt. Express **21**, 23950–23962 (2013).
5. I. Carr and D. Hanna, "Performance of a Nd:YAG oscillator/ampflifier with phase-conjugation via stimulated Brillouin scattering," Appl. Phys. B: Lasers Opt. **36**, 83–92 (1985).
6. I. S. Grudinin, A. B. Matsko, and L. Maleki, "Brillouin lasing with a CaF_2 whispering gallery mode resonator," Phys. Rev. Lett. **102**, 043902 (2009).
7. A. Zadok, A. Eyal, and M. Tur, "Stimulated Brillouin scattering slow light in optical fibers," Appl. Opt. **50**, E38–E49 (2011).
8. D. Garcus, T. Gogolla, K. Krebber, and F. Schliep, "Brillouin optical-fiber frequency-domain analysis for distributed temperature and strain measurements," J. Light. Technol. **15**, 654–662 (1997).
9. A. Motil, A. Bergman, and M. Tur, "State of the art of Brillouin fiber-optic distributed sensing," Opt. & Laser Technol. **78**, 81–103 (2016).
10. Y. Mizuno, W. Zou, Z. He, and K. Hotate, "Proposal of Brillouin optical correlation-domain reflectometry (BOCDR)," Opt. Express **16**, 12148–12153 (2008).
11. S. Liehr, M. Wendt, and K. Krebber, "Distributed strain measurement in perfluorinated polymer optical fibres using optical frequency domain reflectometry," Meas. Sci. Technol. **21**, 094023 (2010).
12. Y. Mizuno and K. Nakamura, "Potential of Brillouin scattering in polymer optical fiber for strain-insensitive high-accuracy temperature sensing," Opt. Lett. **35**, 3985–3987 (2010).

Optics EXPRESS

13. A. Minardo, R. Bernini, and L. Zeni, "Distributed temperature sensing in polymer optical fiber by BOFDA," IEEE Photonics Technol. Lett. **26**, 387–390 (2014).
14. N. Hayashi, Y. Mizuno, and K. Nakamura, "Distributed Brillouin sensing with centimeter-order spatial resolution in polymer optical fibers," J. Light. Technol. **32**, 3397–3401 (2014).
15. H. Lee, N. Hayashi, Y. Mizuno, and K. Nakamura, "Slope-assisted Brillouin optical correlation-domain reflectometry using polymer optical fibers with high propagation loss," J. Light. Technol. **35**, 2306–2310 (2017).
16. S. Liehr, *Fibre Optic Sensing Techniques Based on Incoherent Optical Frequency Domain Reflectometry* (BAM-Dissertationsreihe, 2015).
17. A. Kharaz and B. Jones, "A distributed optical-fibre sensing system for multi-point humidity measurement," Sensors Actuators A: Phys. **47**, 491–493 (1995).
18. P. Kronenberg, P. K. Rastogi, P. Giaccari, and H. G. Limberger, "Relative humidity sensor with optical fiber Bragg gratings," Opt. Lett. **27**, 1385–1387 (2002).
19. S. F. Correia, P. Antunes, E. Pecoraro, P. P. Lima, H. Varum, L. D. Carlos, R. A. Ferreira, and P. S. André, "Optical fiber relative humidity sensor based on a FBG with a di-ureasil coating," Sensors **12**, 8847–8860 (2012).
20. G. Woyessa, K. Nielsen, A. Stefani, C. Markos, and O. Bang, "Temperature insensitive hysteresis free highly sensitive polymer optical fiber Bragg grating humidity sensor," Opt. Express **24**, 1206–1213 (2016).
21. W. Zhang, D. J. Webb, and G.-D. Peng, "Investigation into time response of polymer fiber Bragg grating based humidity sensors," J. Light. Technol. **30**, 1090–1096 (2012).
22. W. Michie, N. Graham, F. Santos, E. Bergqvist, B. Carlstrom, C. Moran, B. Culshaw, I. McKenzie, and M. Konstantakis, "Distributed sensor for water and pH measurements using fiber optics and swellable polymeric systems," Opt. Lett. **20**, 103–105 (1995).
23. P. J. Thomas and J. O. Hellevang, "A fully distributed fibre optic sensor for relative humidity measurements," Sensors Actuators B: Chem. **247**, 284–289 (2017).
24. C. Galindez, F. J. Madruga, and J. M. Lopez-Higuera, "Influence of humidity on the measurement of Brillouin frequency shift," IEEE Photonics Technol. Lett. **20**, 1959–1961 (2008).
25. C. Galindez, F. J. Madruga, and J. M. Lopez-Higuera, "Brillouin frequency shift of standard optical fibers set in water vapor medium," Opt. Lett. **35**, 28–30 (2010).
26. S. Muto, O. Suzuki, T. Amano, and M. Morisawa, "A plastic optical fibre sensor for real-time humidity monitoring," Meas. Sci. Technol. **14**, 746 (2003).
27. S. Liehr, M. Breithaupt, and K. Krebber, "Distributed humidity sensing in PMMA optical fibers at 500 nm and 650 nm wavelengths," Sensors **17**, 738 (2017).
28. H. Bair, G. Johnson, and R. Merriweather, "Water sorption of polycarbonate and its effect on the polymers dielectric behavior," J. Appl. Phys. **49**, 4976–4984 (1978).
29. M. Unemori, Y. Matsuya, S. Matsuya, A. Akashi, and A. Akamine, "Water absorption of poly (methyl methacrylate) containing 4-methacryloxyethyl trimellitic anhydride," Biomaterials **24**, 1381–1387 (2003).
30. P. Stajanca, O. Cetinkaya, M. Schukar, P. Mergo, D. J. Webb, and K. Krebber, "Molecular alignment relaxation in polymer optical fibers for sensing applications," Opt. Fiber Technol. **28**, 11–17 (2016).
31. Y. J. Weitsman, *Fluid Effects in Polymers and Polymeric Composites* (Springer Science & Business Media, 2011).
32. Y. Luo, B. Yan, Q. Zhang, G.-D. Peng, J. Wen, and J. Zhang, "Fabrication of polymer optical fibre (POF) gratings," Sensors **17**, 511 (2017).
33. Y. Koike, *Fundamentals of Plastic Optical Fibers* (John Wiley & Sons, 2014).
34. O. A. Alduchov and R. E. Eskridge, "Improved Magnus form approximation of saturation vapor pressure," J. Appl. Meteorol. **35**, 601–609 (1996).
35. Y. Mizuno, P. Lenke, K. Krebber, and K. Nakamura, "Characterization of Brillouin gain spectra in polymer optical fibers fabricated by different manufacturers at 1.32 and 1.55 um," IEEE Photonics Technol. Lett. **24**, 1496–1498 (2012).
36. Y. Mizuno and K. Nakamura, "Core alignment of butt coupling between single-mode and multimode optical fibers by monitoring Brillouin scattering signal," J. Light. Technol. **29**, 2616–2620 (2011).
37. A. Minardo, R. Bernini, and L. Zeni, "Experimental and numerical study on stimulated Brillouin scattering in a graded-index multimode fiber," Opt. Express **22**, 17480–17489 (2014).
38. Y. Dong, P. Xu, H. Zhang, Z. Lu, L. Chen, and X. Bao, "Characterization of evolution of mode coupling in a graded-index polymer optical fiber by using Brillouin optical time-domain analysis," Opt. Express **22**, 26510–26516 (2014).
39. Y. Mizuno, T. Ishigure, and K. Nakamura, "Brillouin gain spectrum characterization in perfluorinated graded-index polymer optical fiber with 62.5-um core diameter," IEEE Photonics Technol. Lett. **23**, 1863–1865 (2011).
40. A. Schreier, T. Jeschke, K. Petermann, A. Wosniok, and K. Krebber, "Analytical model for mode based insertion loss in ball-lensed coupling of graded-index silica and polymer fibres," in *26th International Conference on Plastic Optical Fibres, POF 2017 - Proceedings,* (2017).
41. K. E. Carroll, C. Zhang, D. J. Webb, K. Kalli, A. Argyros, and M. C. Large, "Thermal response of Bragg gratings in PMMA microstructured optical fibers," Opt. Express **15**, 8844–8850 (2007).
42. K. Minakawa, N. Hayashi, Y. Shinohara, M. Tahara, H. Hosoda, Y. Mizuno, and K. Nakamura, "Wide-range temperature dependences of Brillouin scattering properties in polymer optical fiber," Jpn. J. Appl. Phys. **53**, 042502 (2014).

Optics EXPRESS

43. J. G. Speight, *Lange's Handbook of Chemistry*, vol. 1 (McGraw-Hill New York, 2005).
44. M. R. Moldover, J. M. Trusler, T. Edwards, J. B. Mehl, and R. S. Davis, "Measurement of the universal gas constant R using a spherical acoustic resonator," Phys. Rev. Lett. **60**, 249 (1988).